


# Electron Transport Properties of Diarylethene Photoswitches by a Simplified NEGF-DFT Approach

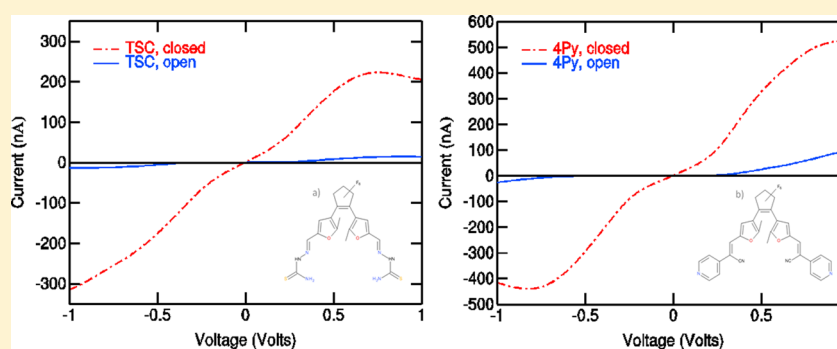
Vincenzo Barone,<sup>†</sup> Ivo Cacelli,<sup>‡</sup> Alessandro Ferretti,<sup>§</sup> and Michele Visciarelli<sup>\*,†,§</sup>

<sup>†</sup>Scuola Normale Superiore, Piazza dei Cavalieri, I-56126 Pisa, Italy

<sup>‡</sup>Dipartimento di Chimica e Chimica Industriale, Università di Pisa, Via Risorgimento 35, 56126 Pisa, Italy

<sup>§</sup>Istituto di Chimica dei Composti OrganoMetallici del CNR UOS di Pisa, Area della Ricerca di Pisa, Via G. Moruzzi 1, I-56122 Pisa, Italy

 Supporting Information



**ABSTRACT:** A homemade program called FOXY has been used for the theoretical investigation on the conducting properties of two diarylethene based molecules, which, according to recent literature data, can act as photoswitches. FOXY uses a simplified method relying on NEGF theory coupled to DFT calculations and using a suitable electric field to mimic the bias voltage, together with a simple representation of the electrodes. The results confirm the experimental findings and are rationalized by analyzing the space extension of the pertinent molecular orbitals in the ON and OFF electronic states and confirm the FOXY program as a cheap and reliable code to be used in the field of molecular electronics.

## 1. INTRODUCTION

The continuous dimensional and functional scaling of MOSFETs (metal-oxide-semiconductor field-effect transistor) is driving information processing technology into a broad spectrum of new applications. Dimensional scaling of MOSFETs will eventually approach fundamental limits, and so several new alternative solutions are being explored to sustain the integrated circuit scaling (governed by the famous Moore's Law<sup>1</sup>) into future times. This is pushing interest in new devices for information processing and memories, showing the same capabilities of MOSFET devices with a constant scaling of the dimension and a reduction of the power usage.

A possible solution to this requirement is to use molecules as the focal element of a new class of devices. The very small dimensions and the electronic properties that should characterize these systems make molecules good candidates to become basic blocks for future electronics. This new scientific field, called molecular electronics, allows chemical engineering of organic molecules with physical and electronic properties tailored by synthetic methods, bringing a new dimension in design flexibility that does not exist in typical inorganic electronic materials.

In the last years, many studies have been dedicated to molecular electronics, from both an experimental and a

theoretical point of view. From the theoretical and computational sides, the development of specific models and methodologies, ranging from time-independent<sup>2–6</sup> to time-dependent<sup>7–11</sup> transport schemes and mainly based on Green's function methods, has provided valuable tools to tackle at different level of approximation the problem of charge transport in single molecules. Green's function methods are starting to be widely used also by device engineers due to their versatility because these methods can be adopted for calculating current transport both in single molecules and in novel semiconductor nanostructures alike and, consequently, tailoring new devices on specific needs. Despite this effort, a direct comparison between computed single-molecule *I*–*V* characteristics and experimental data is still difficult to be achieved, and often the discrepancy is one or two orders of magnitude.<sup>12,13</sup> This may find an explanation in the complexity of the contact geometry between the molecule and the electrodes, which governs their interaction. In addition, there are still several issues inherent to the theory, such as the role of nuclear degrees of freedom and many-body effects.<sup>14–16</sup>

**Received:** February 27, 2014

**Revised:** April 13, 2014

**Published:** April 16, 2014

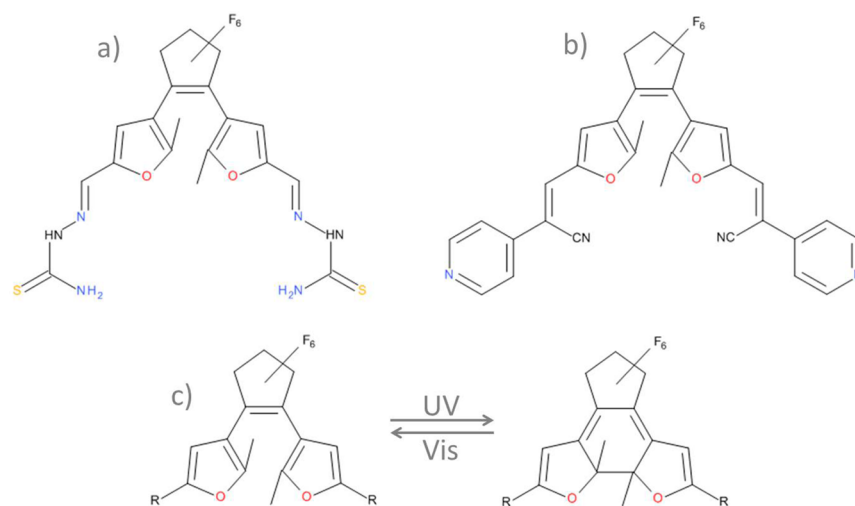


**Figure 1.** (a) TSC and (b) 4Py molecules. (c) Open and closed forms of the diarylethene unit.<sup>26</sup> The diarylethene unit changes, reversibly, between open and closed forms via visible and UV radiation. R indicates a generic end group.

Molecular switches are devices where the electron flow, which can be mono- or bi-directional, can be activated (ON) or deactivated (OFF) through an external action (gate). These are three-terminal devices where the external stimulus can be electrical, for example, a voltage applied to the gate,<sup>17,18</sup> or even optical, providing that the molecule is photoactive. In this case, the energy of the incident radiation can be used to change the conformation of the molecule, from a conducting one to a nonconducting one, and vice versa. When the switching functionality is activated by an external optical radiation, we speak of molecular optical switches. These species undergo a reversible transformation between two stable states showing different equilibrium geometry and physical properties.

This is the case of species based on azobenzene<sup>17,19–21</sup> or diarylethene<sup>17,20,22–26</sup> groups, where the easiness of controlling reversibility at the molecular level and the fast response time to input optical signals can be a significant advantage in view of possible technological use in real devices. Indeed, there are already promising applications in memory elements<sup>27</sup> and studies that point out the possibility of building transistor-like devices<sup>28</sup> using optically active molecules. In conclusion, photochromic molecules can grant access to optical switches and memories and therefore meet the requirements for today's surge to design all-optical computers.

In this work, we focus on diarylethenes, where a variation on the conductance can be expected as a consequence of the photoinduced rearrangement of single and double bonds inside the central ring (Figure 1). This class of molecules has, in fact, two isomers: one with a C–C open bond and one with the same bond closed. By irradiation with UV light the open form gives rise to the closed form, which, in turn, transforms back into the open form by visible-light irradiation. Experimentally,<sup>24,26</sup> open and closed forms have been found to exhibit rather different conductivity. In particular, we are interested in the TSC and 4Py species displayed in Figure 1, as defined in the original work of Briechle et al., which were shown to have an ON state with a current of two orders of magnitude higher than the OFF state.

## 2. THEORETICAL METHOD

From a theoretical point of view, the transport process through a single molecule is essentially viewed as electrons, prepared in

reservoirs at different electrochemical potentials, that scatter through a central region from one electrode to the other. Most of the theoretical work on the subject of nanoscale and molecular transport is based on Landauer–Büttiker theory<sup>29</sup> coupled to non-equilibrium Green's function (NEGF) method and density functional theory (DFT). The calculation of the fundamental quantities relies on a modified self-consistent DFT calculation, which is usually cumbersome and time-consuming, both for the calculation of the optimal geometry of the molecule/electrodes junction and for ground-state calculations. Therefore, fast and reliable techniques are needed which, focusing on the contacted molecule, may give reliable response on its conduction properties as well as on its functional role in the device. The goal is to set up a low-cost computational approach that may be applied with confidence to a large variety of devices, simplifying the metal–molecule interaction while retaining all essential physics of the charge transport due to the molecular bridge. The method used in the present work is basically a simplified version of the aforementioned Landauer–Büttiker–NEGF method. It is based on a paper of Gonzalés et al.<sup>30</sup> and has been implemented in a homemade Fortran code named FOXY, which has been successfully employed in the study of bipyridine-based molecular switches<sup>31</sup> and molecular rectifiers.<sup>32</sup> The main idea beneath the model is to focus on the response of the contacted molecule to the voltage bias rather than to the details of the contact itself, taking the molecule-lead coupling as proportional to the projection of the molecular orbitals onto suitable terminal fragments bound to the central molecule. Such projections can be easily computed by the molecular orbitals as arising from a suitable one-particle effective Hamiltonian of the extended molecule, obtained by adding a three-atom Gold cluster at both the left and the right ends of the molecule. The geometry is chosen to model the most probable contact between the molecule and Au(111) surface, which is with the sulfur or nitrogen atom in hollow position with respect to the gold atoms, with Au–Au and Au–S distances as 2.88 and 2.82 Å, respectively.<sup>33</sup> The projection terms and the corresponding coupling terms can then be used to calculate the transmission function  $T(E,V)$  and the total current. (See Supporting Information and refs 31, 32, and 34 for details.) In the model, we have introduced an empirical constant  $\Delta$ , which modulates the molecule–lead interaction

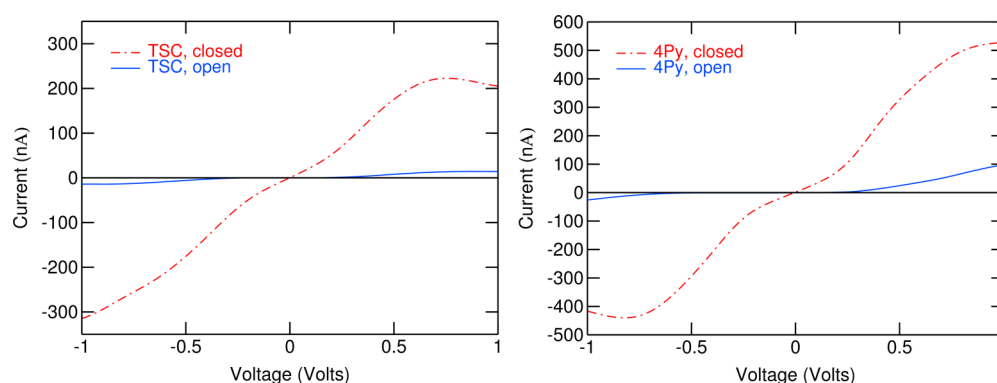


**Figure 2.** Current–voltage characteristics of the TSC (left) and 4Py (right), in both the ON and OFF states.

strength, whose values were already calibrated in a previous work.<sup>32</sup> The calibration was based on the reproduction of the experimental  $I$ – $V$  curves of the prototypical benzene 1,4-dithiol bound to two gold electrodes as in the seminal work of Reed et al.<sup>35</sup> We found  $\Delta = 0.0015$  eV to be a reasonable value. Another important issue to be addressed is the evaluation of the Fermi level of the entire system, which affects the calculation of the total current. Usually, the Fermi level of the entire electrode plus the molecule junction is located somewhere inside the HOMO–LUMO gap of the central molecule.<sup>36</sup> However, in many theoretical works the Fermi level of bulk Gold ( $-5.3$  eV) is used (since gold is the most used material in molecular junction experiments). When dealing with large chunks of electrodes, this choice is justified by the “total” shifting effect generated by the interaction of the molecule with full semi-infinite leads. Because in the present model only a small part of the electrode is explicitly included, the bulk gold Fermi level is found in some cases below the HOMO level. Noticing that the transmission function is independent of the position of the Fermi level and can be considered as the reference quantity on an absolute energy scale, we use, as Fermi level, the midpoint of the HOMO and LUMO orbital energies.

In the FOXY model, the effect of the external voltage onto the electronic states of the extended molecule is treated as the bias applied between the two leads, giving rise to an uniform electric field parallel to the transport axis, like the one generated by a capacitor whose plates are semi-infinite electrodes. The voltage applied to this “effective” capacitor is the external voltage  $V$ , with distance between the plates equal to the distance of the two small ending metal clusters mimicking the full semi-infinite electrodes.

The entire computational cost of the method is very low and mostly concentrated in the DFT calculation of ground-state properties of the extended molecule (one for each voltage, which is to be analyzed). The method is fast and versatile: many types of molecules with different functionalities can be probed, using any metal for the few atoms of the leads included in the calculation. All of these characteristics imply the possibility for engineers, physicists, and chemists to use it as a tool for a preliminary screening of a large number of molecules, which may have interesting properties from the electronic transport point of view. In the presence of a large set of molecules to be probed by experimental methods, we believe that the FOXY model can help identifying the most promising species beforehand.

The FOXY code has recently been incorporated in the Gaussian 09 program;<sup>37</sup> it does not require the modification of

the usual self-consistent scheme because here the calculation of the transmission function and the total current only needs the knowledge of eigenvalues and eigenfunctions of the extended molecule (even in cases with the inclusion of an external electrical field) and can be performed after the standard self-consistent DFT procedure. All the starting quantities needed for the transport calculations can be easily obtained from a standard ground-state DFT calculation (or from any other mean-field single-particle calculation).

For this work, all ground-state calculations, as long as the geometry optimization at zero bias, have been performed at the DFT/B3LYP level, with 6-311\*G basis sets for all atoms, except for S and Au (which employed LANL2DZ basis set). Also, separate calculations were made for every voltage point (with appropriate electric field) at the same level of theory.

### 3. RESULTS AND DISCUSSION

The computed  $I$ – $V$  curves for the TSC and 4Py species, in both open and closed states, are reported in Figure 2. For all computations, the bias voltage range investigated has been covered by 20 points, one each 0.1 V. For both systems, we find a much higher conduction for the closed form (Figure 1). The current is found larger, both in the ON and in the OFF states, for the 4Py species, and at small bias we can recognize an Ohmic behavior, which agrees with the experiments.<sup>24</sup> The  $I$ – $V$  curves also show slightly asymmetric currents for positive and negative voltages, as the asymmetry of the molecules found in the geometrical optimization would suggest, especially in the open state.

As far as the 4Py species is concerned, the  $I$ – $V$  characteristics are in accordance with the experiments,<sup>24</sup> whereas for the TSC system, the literature data available seem to give different and contrasting results. In fact, whereas in ref 24 the TSC system is shown to behave as the 4Py, with the closed state conducting and the open one not, in ref 26, it is the open state that shows larger conductance. Our results point toward an analogous behavior of the systems considered in ref 24, which is supported by a comparison of the electronic structure of the open and closed forms, as discussed later. In terms of a quantitative comparison between our calculations and the experiments, we can say that we find, as in ref 24, that the current for the 4Py species is roughly three times that for the TSC system. With respect to ref 24, we find values three orders of magnitude larger but in good quantitative agreement with those of ref 26. Such inconsistency in the experiments would indeed require further investigation, which is out of our competencies.

The  $I$ – $V$  behavior of Figure 2 can be explained by looking at the transmission functions  $T(E)$  of Figures 3 and 4 because, as

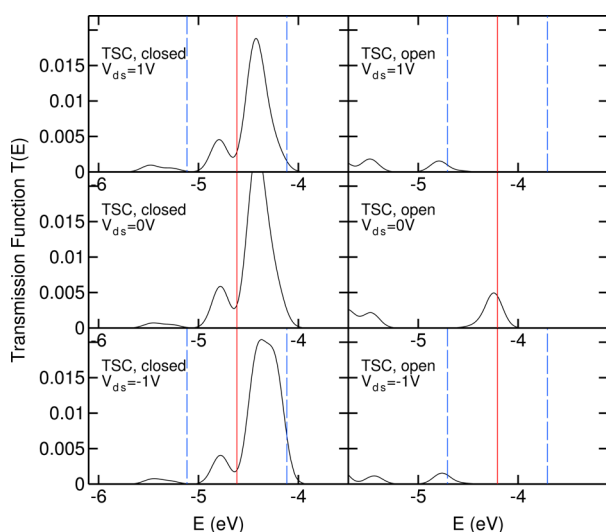


**Figure 3.** Transmission function of the TSC species, in both “open” (right column) and “closed” (left column) conformations, at +1, 0, and –1 V. Vertical red line: Fermi level of the species. Vertical blue lines: integration range.

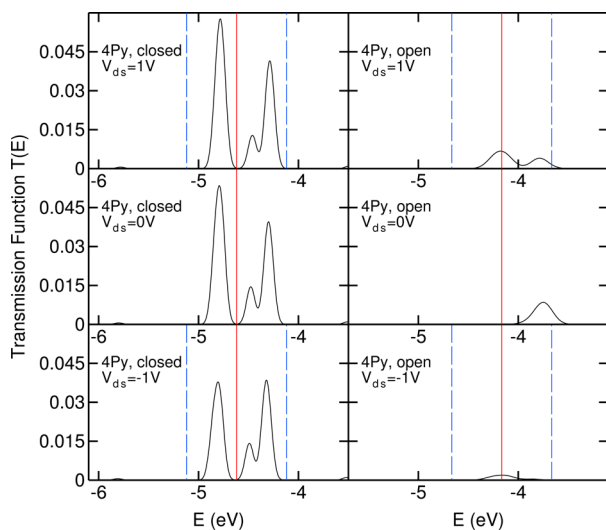


**Figure 4.** Transmission function of the 4Py species in both “open” (right column) and “closed” (left column) conformations at +1, 0, and –1 V. Vertical red line: Fermi level of the species. Vertical blue lines: integration range.

of Landauer theory, the current can be expressed as (see also the Supporting Information):

$$I(V) = \frac{2e}{h} \int_{\mu_L}^{\mu_R} T(E, V) dE$$

As previously outlined, the Fermi level is taken in the middle of the HOMO–LUMO orbital energies (red vertical line in the Figures), and the transmission function is dimensionless.

The orbitals that have significant projection onto the terminal Gold fragments and give rise to significant peaks in the transmission function within the  $[-0.5$  V,  $+0.5$  V] bias window are the HOMO, LUMO, and LUMO+1. For the TSC species in closed form (Figure 3, left), LUMO and LUMO+1

provide the largest contribution to the  $T(E)$  functions, with a wide peak generated by the broadening of these two levels, whereas for the 4Py species (Figure 4, left), the contribution of the three aforementioned orbitals appears more balanced, and even the HOMO gives an important contribution to the conductance, especially for positive bias. From this analysis, it seems that for the 4Py the conduction is of electron–hole type due to the fact that both occupied and virtual orbitals are involved in the conduction process. This is in contrast with the TSC species, where only virtual orbitals are involved, and the conduction can then be thought of as electron-type only.

The difference in the  $T(E)$  between the open and the closed forms of both TSC and 4Py species is rather evident by comparing left and right parts of Figures 3 and 4: the peaks of the open form are at least one order of magnitude smaller than in the open case. This results in a small or negligible current observed for both of the open forms. In particular, for the open TSC system, only a small part of the bands of  $T(E)$  fall within the integration range (marked by dashed vertical lines), and the current is then very low. We should also notice that for the closed species the applied field has a negligible effect on the energy position of the MOs, which are almost unchanged at –1, 0, and +1 V (especially in the 4Py case). Moreover, the small dependence of the peak intensity of the outer shell MOs in  $T(E)$  indicates that their projection on the terminal fragment is almost constant at the considered voltages. These observations lead to the conclusion that there are no significant polarization effects at the origin of the computed  $I$ – $V$  characteristics.

Further insights into the transport properties of the two species can be obtained by a closer look at the shape of the molecular orbitals, which are relevant for the conduction mechanism. In Figures 5 and 6, HOMO, LUMO, and LUMO +1 at 0 V for the TSC and 4Py molecules, in either the open and closed states, are reported. We can see that in the ON state (closed form) the MOs are essentially delocalized in the whole molecule, with significant component on both the terminal Au fragments: the HOMO has the largest molecule-type character, whereas the virtual orbitals have mostly gold character. When the external radiation, opening the central bond of the diarylethene moiety, switches the system from the closed to the open state, the MOs near the Fermi level lose their delocalized character and become localized separately in the left and right parts of the extended molecule. Localized orbitals cannot provide good transmission channels for an electron to tunnel from one electrode to the other, mainly because they do not have significant components on both left and right Au fragments and therefore originate small molecule–electrode couplings and minimal peaks in the transmission function. As a consequence, the current is very low in the open form, as previously detailed.

#### 4. CONCLUSIONS

In conclusion, we have investigated charge transport in the TSC and 4Py photochromic species based on a central sulfur-free diarylethene core. The global behavior observed experimentally for these photochromic switches<sup>24,26</sup> has been successfully reproduced within the framework of a simplified NEGF–Landauer transport theory. A rationale of the observed characteristics of both open and closed states may be given by linking the transmission functions with the shape of the relevant molecular orbitals, which are delocalized in the closed



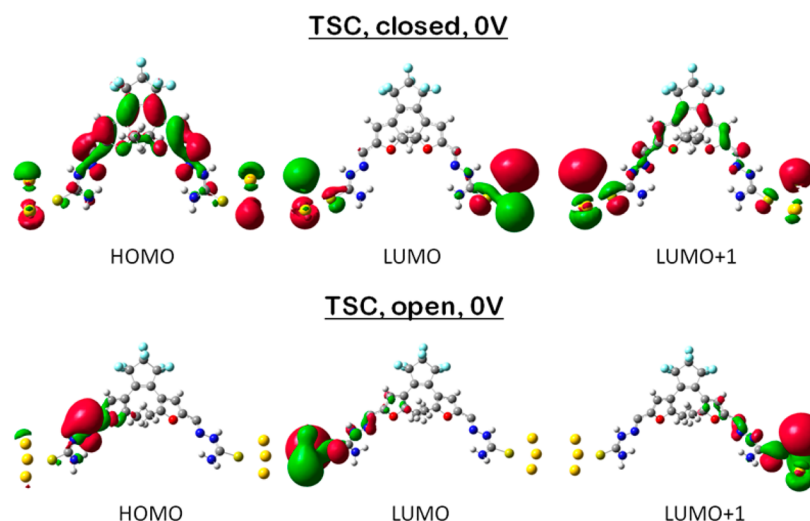


**Figure 5.** MOs of the TSC molecule relevant for the conduction at zero bias.

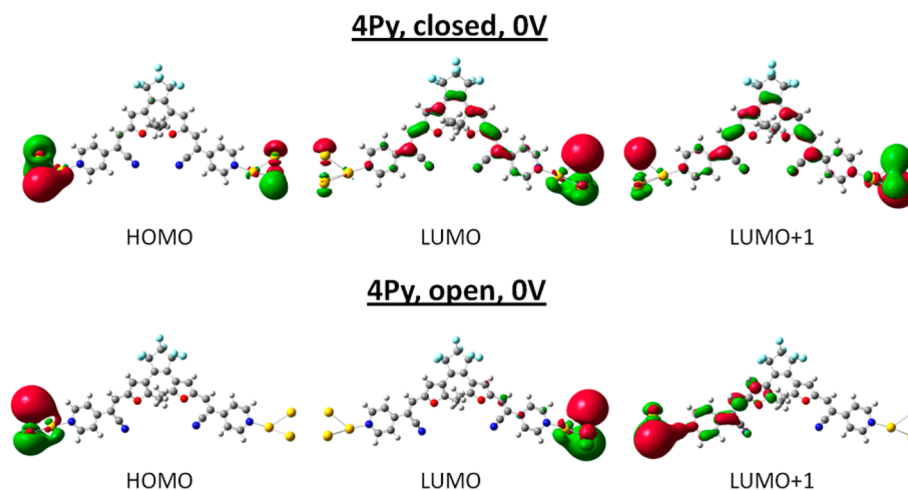


**Figure 6.** MOs of the 4Py molecule relevant for the conduction at zero bias.

state and strongly localized in the open state, with drastic consequences in the peak intensity.

The method here discussed and implemented in our code FOXY represents a simple cost-effective computational approach for future molecular device engineering and can be used as a tool for rapid evaluation of electrical behavior of molecules of interest in the field of molecular electronics.

## ■ ASSOCIATED CONTENT

### 📄 Supporting Information

Full detailed description of the theoretical method implemented in the FOXY code. This material is available free of charge via the Internet at <http://pubs.acs.org>.

## ■ AUTHOR INFORMATION

### Corresponding Author

\*E-mail: [viscio85@gmail.com](mailto:viscio85@gmail.com), [michele.visciarelli@sns.it](mailto:michele.visciarelli@sns.it).

### Notes

The authors declare no competing financial interest.

## ■ REFERENCES

- (1) Moore, G. *Electronics* **1965**, 114–117.
- (2) Rocha, A. R.; Garcia Suárez, V. M.; Bailey, S.; Lambert, C.; Ferrer, J.; Sanvito, S. *Phys. Rev. B* **2006**, 73 (8), 085414.
- (3) Stokbro, K.; Taylor, J.; Brandbyge, M. *J. Am. Chem. Soc.* **2004**, 125 (13), 3674–3675.
- (4) Xue, Y.; Datta, S.; Ratner, M. A. *Chem. Phys.* **2002**, 281, 151.
- (5) Lang, N. D.; Di Ventra, M. *Phys. Rev. B* **2001**, 65, 045402.
- (6) Garcia Suárez, V. M.; Ferrer, J. *Phys. Rev. B* **2012**, 86 (12), 125446.
- (7) D'Agosta, R.; Di Ventra, M. *Phys. Rev. B* **2008**, 78, 165105–165120.
- (8) Di Ventra, M.; D'Agosta, R. *Phys. Rev. Lett.* **2007**, 98, 226403–226406.
- (9) Sánchez, C. G.; Stamenova, M.; Sanvito, S.; Bowler, D. R.; Horsfield, A. P.; Todorov, T. N. *J. Chem. Phys.* **2006**, 124, 214708.
- (10) Stefanucci, G.; Kurth, S.; Gross, E. K. U.; Rubio, A. *Theor. Comput. Chem.* **2007**, 17, 247–264.
- (11) Yam, C. Y.; Zheng, X.; Chen, G.; Wang, Y.; Frauenheim, T.; Niehaus, T. A. *Phys. Rev. B* **2011**, 83, 245448.
- (12) Nitzan, A.; Ratner, M. A. *Science* **2003**, 300, 1384.
- (13) Lindsay, S.; Ratner, M. A. *Adv. Mater.* **2007**, 19, 23.
- (14) Myöhänen, P.; Stan, A.; Stefanucci, G.; van Leeuwen, R. *Phys. Rev. B* **2009**, 80, 115107.
- (15) Galperin, M.; Ratner, M. A.; Nitzan, A. *J. Phys.: Condens. Matter* **2007**, 19, 103201.
- (16) Härtle, R.; Benesch, C.; Thoss, M. *Phys. Rev. Lett.* **2009**, 102, 146801.

- (17) van der Molen, S. J.; Liljeroth, P. *J. Phys.: Condens. Matter* **2010**, *22*, 133001.
- (18) Song, H.; Reed, M. A.; Lee, T. *Adv. Mater.* **2011**, *23* (14), 1583–1608.
- (19) Beharry, A. A.; Woolley, G. A. *Chem. Soc. Rev.* **2011**, *40*, 4422–4437.
- (20) Kudernac, T.; Katsonis, N.; Brune, W. R.; Feringa, B. L. *J. Mater. Chem.* **2009**, *19*, 7168–7177.
- (21) Henzi, J.; Puschnig, P.; Ambrosch-Draxl, C.; Schaate, A.; Ufer, B.; Behrens, P.; Morgenstern, K. *Phys. Rev. B* **2012**, *85* (3), 035410.
- (22) Cheng, H.-B.; Zhang, H.-Y.; Liu, Y. *J. Am. Chem. Soc.* **2013**, *135* (28), 10190–10193.
- (23) Uchida, K.; Yamanoi, Y.; Yonezawa, T.; Nishihara, H. *J. Am. Chem. Soc.* **2011**, *133* (24), 9239–9241.
- (24) Kim, Y.; Hellmuth, T. J.; Sysoiev, D.; Pauly, F.; Pietsch, T.; Wolf, J.; Erbe, A.; Huhn, T.; Groth, U.; Steiner, U. E.; Scheer, E. *Nano Lett.* **2012**, *12* (7), 3736–3742.
- (25) Simão, C.; Mas-Torrent, M.; Casado-Montenegro, J.; Otón, F.; Veciana, J.; Rovira, C. *J. Am. Chem. Soc.* **2011**, *133* (34), 13256–13259.
- (26) Briechele, B. M.; Kim, Y.; Ehrenreich, P.; Erbe, A.; Sysoiev, D.; Huhn, T.; Groth, U.; Scheer, E. *Beilstein J. Nanotechnol.* **2012**, *3*, 798–808.
- (27) Uchida, K.; Saito, M.; Murakami, A.; Kobayashi, T.; Nakamura, S.; Irie, M. *Chem.—Eur. J.* **2005**, *11*, 534–542.
- (28) Gilat, S. L.; Kawai, S. H.; Lehn, J. M. *Chem.—Eur. J.* **1995**, *1*, 275–284.
- (29) Landauer, R. *IBM J. Res. Dev.* **1957**, *1* (3), 223–231.
- (30) Gonzalés, C.; Simon-Manso, Y.; Batteas, J.; Marquez, M.; Ratner, M. A.; Mujica, V. *J. Phys. Chem. B* **2004**, *108*, 18414.
- (31) Barone, V.; Cacelli, I.; Ferretti, A.; Visciarelli, M. *Phys. Chem. Chem. Phys.* **2013**, *15*, 11409.
- (32) Barone, V.; Cacelli, I.; Ferretti, A.; Visciarelli, M. *Chem. Phys. Lett.* **2012**, *549*, 1–5.
- (33) Franzen, S. *Chem. Phys. Lett.* **2003**, *381*, 315.
- (34) Cacelli, I.; Ferretti, A.; Girlanda, M.; Macucci, M. *Chem. Phys.* **2007**, *333*, 26–36.
- (35) Reed, M. A.; Zhou, C.; Muller, C. J.; Burgin, T. P.; Tour, J. M. *Science* **1997**, *278*, 252.
- (36) Zahid, F.; Ghosh, A. W.; Paulsson, M.; Polizzi, E.; Datta, S. *Phys. Rev. B* **2004**, *70* (24), 245317.
- (37) Frisch, M. J.; Trucks, G. W.; Schlegel, H. B.; Scuseria, G. E.; Robb, M. A.; Cheeseman, J. R.; Scalmani, G.; Barone, V.; Mennucci, B.; Petersson, G. A.; Nakatsuji, H.; Caricato, M.; Li, X.; Hratchian, H. P.; Izmaylov, A. F.; Bloino, J.; Zheng, G.; Sonnenberg, J. L.; Hada, M.; Ehara, M.; Toyota, K.; Fukuda, R.; Hasegawa, J.; Ishida, M.; Nakajima, T.; Honda, Y.; Kitao, O.; Nakai, H.; Vreven, T.; Montgomery, J. A., Jr.; Peralta, J. E.; Ogliaro, F.; Bearpark, M.; Heyd, J. J.; Brothers, E.; Kudin, K. N.; Staroverov, V. N.; Kobayashi, R.; Normand, J.; Raghavachari, K.; Rendell, A.; Burant, J. C.; Iyengar, S. S.; Tomasi, J.; Cossi, M.; Rega, N.; Millam, J. M.; Klene, M.; Knox, J. E.; Cross, J. B.; Bakken, V.; Adamo, C.; Jaramillo, J.; Gomperts, R.; Stratmann, R. E.; Yazyev, O.; Austin, A. J.; Cammi, R.; Pomelli, C.; Ochterski, J. W.; Martin, R. L.; Morokuma, K.; Zakrzewski, V. G.; Voth, G. A.; Salvador, P.; Dannenberg, J. J.; Dapprich, S.; Daniels, A. D.; Farkas, Ö.; Foresman, J. B.; Ortiz, J. V.; Cioslowski, J.; Fox, D. J. *Gaussian 09*; Gaussian, Inc.: Wallingford, CT, 2009.